The role of carbides in the hydrogen induced mechanical degradation of steels

Tom DEPOVER, Aurélie LAUREYS, Tim DE SERANNO, Lisa CLAEYS, Emilie VAN DEN EECKHOUT and Kim VERBEKEN

Ghent University, Zwijnaarde, Belgium, tom.depover@ugent.be, aurelie.laureys @ugent.be, tim.deseranno @ugent.be, lisa.claeys @ugent.be, emilie.vandeneeckhout@ugent.be, kim.verbeken@ugent.be

Abstract:

Carbides offer an important tool in the microstructural design of steels to increase the material's resistance to hydrogen (H) induced mechanical degradation. Carbides can trap H that is absorbed in the material, as such decreasing the amount of mobile or diffusible H, which is known to play an important role in the H induced ductility loss. However, the exact role of the carbides depends very much on the type and shape of carbide, and other characteristics such as coherency, carbide size and size distribution. Moreover, the specific characteristics of the steel matrix in which the carbide is embedded may also play a role.

In the present work, two types of carbides are compared: Ti-based and V-based carbides. For this purpose, two base alloys were used, namely lab cast Fe-C-Ti and Fe-C-V alloys. Appropriate thermal treatment assured varying both the microstructure (as quenched, quenched and tempered (Q&T) and ferritic) as well as the carbide characteristics. These carbide characteristics were evaluated via transmission electron microscopy. Optical microscopy and scanning electron microscopy contributed to the microstructural analysis as well. Furthermore, the material/H interaction was also fully characterized. After in-situ H pre-charging, tensile tests were performed to evaluate the susceptibility to hydrogen embrittlement (HE). The H trapping capacity of the precipitates was investigated by thermal desorption spectroscopy, whereas hot/melt extraction was executed to determine the amount of diffusible and total H present after cathodic H charging.

The performed systematic study clearly demonstrated that the sensitivity of a material to H induced mechanical degradation was influenced by its microstructural characteristics. E.g.:
- The ability to trap H in a Q&T microstructure decreases with carbide size,
- H is effectively trapped at the interface between carbide and matrix for Fe-C-Ti and Fe-C-V and inside carbon vacancies in V_4C_3 precipitates.
- The HE degree increases with measured amount of H for Fe-C-Ti, while the effective trapping sites play an important role for Fe-C-V.
- Both alloys with a ferritic microstructure are very prone to HE due to their high H mobility although low amounts of H are present.
- Carbide size and hence coherency determines mainly the trapping ability of the Ti and V based precipitates, while larger carbo-nitrides are responsible for H induced failure and hence not desirable for alloy design.

Keywords: hydrogen embrittlement; Ti and V based carbides; ferrite; martensite; thermal desorption spectroscopy

Introduction

Hydrogen (H) has a detrimental effect on the mechanical properties of steel since H induces a loss in ductility, often quoted as hydrogen embrittlement (HE). The phenomenon has been reported to impede the development of high strength steels [1]. These steels, often containing a complex multiphase microstructure, are even more prone to H induced mechanical damage [2-4]. Their interaction with H has been studied thoroughly during the last decade [5-7]. Recently, our research group at Ghent University presented results on four high strength steels, i.e. a dual phase (DP), transformation induced plasticity (TRIP), ferrite-bainite (FB) and high strength low alloy steel (HSLA) [8-13]. The H induced mechanical degradation was specifically studied in [4] and a considerable H induced ductility loss was observed, except for the HSLA steel, which was attributed to the presence of Ti- and Nb- carbo-nitrides.
Although HE was first discussed in 1875 by Johnson [14], no complete understanding of the underlying mechanisms has been obtained so far. Next to the H content in the materials, also the mobility of H in different microstructures is a key factor determining the HE susceptibility [4, 15, 16]. Therefore, the synergetic effect of both the H content and H diffusivity was discussed in [15]. The HE degree was evaluated in different microstructures containing a varying amount of H. By decreasing the cross-head deformation speed of the in-situ H charged tensile tests of two bainitic materials with varying carbon content, the importance of H diffusion was confirmed. The increase in HE% with decreasing tensile test speed was higher for the lower H containing bainitic grade due to its higher diffusion coefficient, as determined by permeation experiments [15, 16]. Moreover, pure iron showed a HE% of about 46% although small H amounts, i.e. 0.71 wppm diffusible H, were present in the sample. This was also correlated to the high H diffusivity of the material [15].

This combined effect was also confirmed in the work performed on Fe-C-X alloys [17-20]. Ti, Cr, Mo and V were added as ternary alloying element. The concept of ‘mobile H’ was introduced as H which was trapped at dislocations and effused easily from the H saturated sample. An increase of this mobile H was clearly linked to an increase in HE for the Fe-C-X alloys, especially when plastic deformation occurred. This further confirmed the importance of an enhanced dislocation mobility in the presence of H, which is a experimental indication of the H enhanced localized plasticity (HELP) mechanism. This research was performed since the role of carbides has been relevant in steel alloy development. On the one hand, they induce material strenghtening due to precipitation hardening and, on the other hand, precipitates are mentioned to be beneficial as efficient deep H trapping sites. Consequently, H loses its mobility, which is assumed to be responsible for the detrimental effect of H. Although thermal desorption spectroscopy (TDS) studies showed the H trapping ability of several carbides [21-28], an experimental approach relating their effect to the H effect on the mechanical behavior is limited [29, 30].
Nevertheless, trapping mobile H by well-designed carbides is generally supposed to be the main strategy to enhance the resistance against HE [4, 29, 31]. The multiphase microstructure however impedes the interpretation of the H related data. Therefore, these generic Fe-C-X alloys were recently considered. Next to the impact of carbides, the matrix in which they are embedded plays an important role as well since both the H amount and the H diffusivity play a key role to understand the H induced ductility loss [15-20]. The latter is mainly dependent on the matrix and the embedded trapping sites. Therefore, two different microstructures were considered to evaluate the trapping effect of carbides: a ferritic and a martensitic matrix. The present study aims to compare the different carbides in different microstructures to draw general conclusions in terms of their effect on the H induced mechanical degradation.

Experimental procedure

Two generic Fe-C-X alloys with a stoichiometric amount of a ternary alloying element X were processed (cf. Table 1). Ti and V were added as carbide forming element. These materials were cast, hot rolled and subsequently heat treated to obtain the desired microstructure with embedded Ti and V based precipitates. At first, a martensitic microstructure was aimed for. The alloys were austenitized at 1250°C for 10 minutes followed by a brine water quench. This first condition will be referred to as "as-Q". Besides, a tempering treatment was applied to introduce precipitates in this martensitic microstructure. Secondary hardening due to the precipitation of carbides was optimal at 600°C. The hardness profiles versus tempering temperature can be found in [19, 20]. This second condition will be referred to as "Q&T". Tempering times of 1 and 2 hours were applied to evaluate the effect of the carbide's size and coherency on the trapping ability of the tempered induced particles. The microstructures were studied by optical microscopy, scanning electron microscopy (SEM) and transmission electron microscopy (TEM). The degree of H induced mechanical degradation and the H content were determined, TDS measurements and permeation experiments were performed as described in detail in [19, 20]. For more details on the experimental data, we refer to the corresponding publications [19, 20].

Table 1: *Chemical compositions of the Fe-C-X alloys.*

Alloy Fe-C-X	**wt.% C**	**wt.% X**	**Other elements**
Fe-C-Ti	0.10	0.38	Al: 200-300 wt. ppm
Fe-C-V	0.10	0.57	Other elements: traces

The H/material interaction tests were done on H saturated samples by pre-charging the materials in a 1g/L thiourea 0.5 M H_2SO_4 solution at a current density of 0.8 mA/cm^2 for 1 hour. Hot/melt extraction was performed to determine the H content. The samples were analysed about one minute after H charging and the measurements were done at 1600°C and 300°C to determine the total and diffusible H content respectively. TDS was done to identify the H trapping sites. Therefore, three different heating rates were used (200°C/h, 600°C/h and 1200°C/h). The applied TDS procedure required one hour between the end of H charging and the start of the TDS measurement as a sufficient vacuum needs to be created in the analysis chamber. H electrochemical permeation tests were performed to determine the H diffusion coefficient. The two compartments were filled with a 0.1 M NaOH solution. The H entry side acted as the cathode by applying a current density of 3 mA/cm^2 while the H exit side (anode) was potentiostatically kept constant at -500 mV vs. Hg/$HgSO_4$ reference electrode. The degree of H induced mechanical degradation was determined as:

$$\%HE = 100 \cdot \left(1 - \frac{\varepsilon_{ch}}{\varepsilon_{un}}\right)$$

with ε_{ch} and ε_{un} being the elongation of the H charged and uncharged tensile sample, respectively. Hence, the %HE varies between 0 and 1, with 0 meaning that there is no ductility loss and the material is insensitive to HE. When an index of 1 is obtained, the ductility drop is 100% and HE is maximal. The tensile sample geometry is presented in Fig. 1.

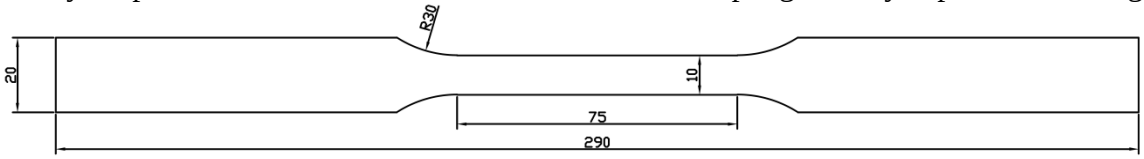

Fig. 1*: Tensile sample geometry in mm.*

Materials characterization

A clear martensitic and Q&T microstructure was observed by optical microscopy. The as-Q condition of the Fe-C-Ti alloy still showed carbides since austenitizing at 1250°C was not sufficient to dissolve all carbides present from casting and rolling (cf. Fig. 2 and Fig. 3 (a)). On the contrary, all carbides of the Fe-C-V alloy were dissolved at 1250°C (cf. Fig. 2). The amount of dissolved C was determined based on thermo-dynamical calculations. Carbides were introduced during tempering for the Q&T condition. TEM images were taken to confirm their presence as presented in Fig. 3 (b-e). Small carbides with sizes less than 10 nm were revealed for the Ti- and V-alloy in the Q&T condition. Their size increased when two hours of tempering was applied. More microstructural details and diffraction patterns for the different carbides (TiC, V_4C_3) can be found in the corresponding publications [19, 20].

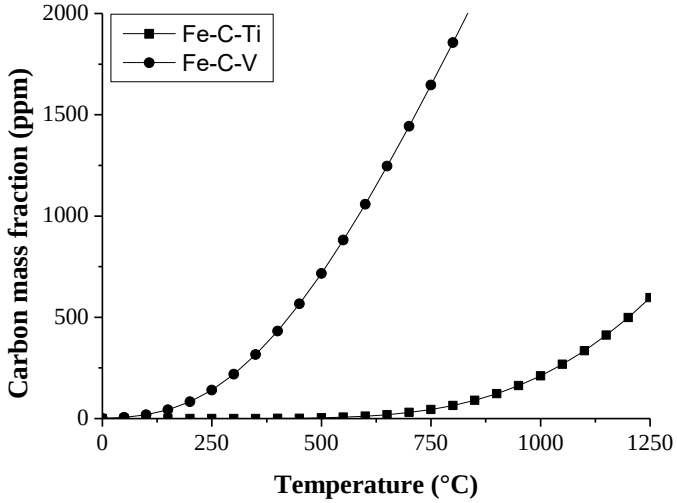

***Fig. 2**: Mass fraction of carbon (ppm) vs. temperature (°C) that can be kept in solid solution at each temperature for stoichiometric total contents of C and Ti or V.*

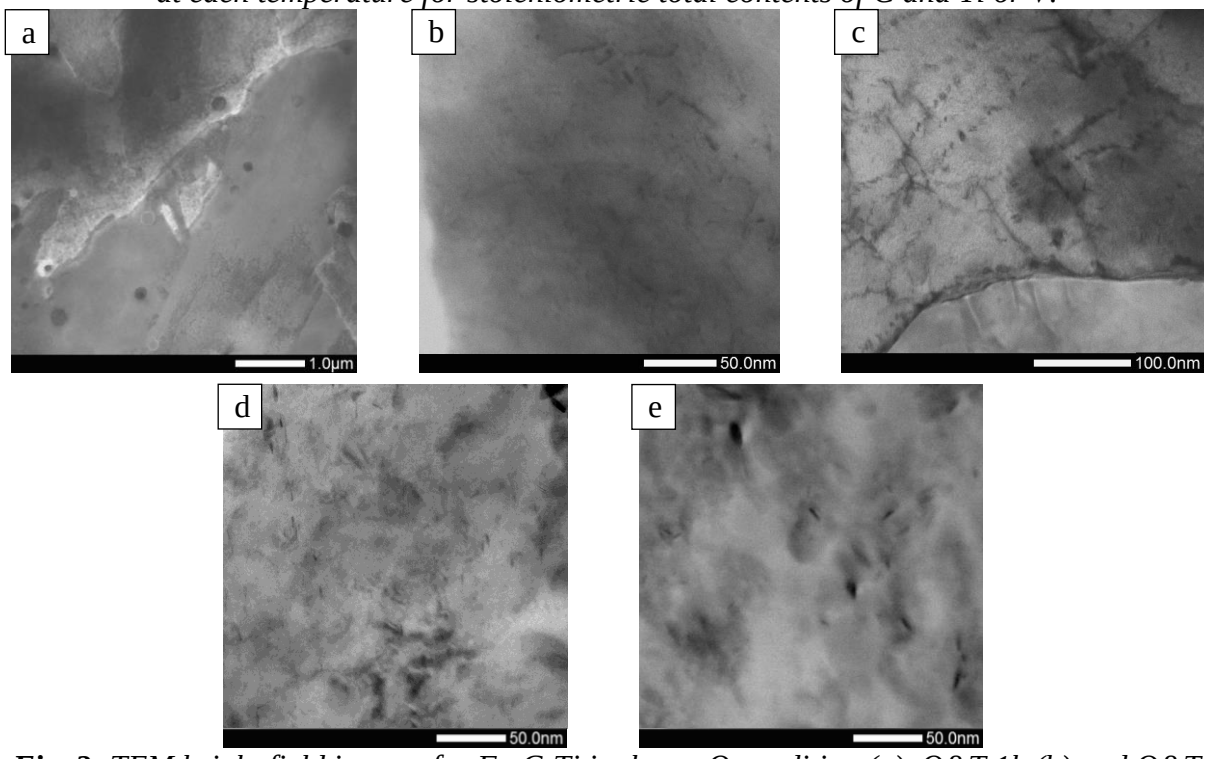

***Fig. 3**: TEM bright field images for Fe-C-Ti in the as-Q condition (a), Q&T 1h (b) and Q&T 2h (c) and for Fe-C-V in the Q&T 1h (d) and Q&T 2h (e) condition.*

Hydrogen induced mechanical degradation

The impact of H on the mechanical behaviour was demonstrated by in-situ tensile testing on both uncharged and H saturated specimen. The stress-strain curves for Ti- and V-alloy in the as-Q, Q&T 1h and Q&T 2h conditions are depicted in Fig. 4. A significantly different HE susceptibility was observed. Tempering resulted in an increase in strength level and ductility for the Fe-C-Ti alloy, while a reduction for both was observed for Fe-C-V although low plastic deformation was present since carbides dissolved fast during austenitizing resulting in a dense carbon rich martensitic microstructure and a more brittle material (cf. Fig. 2). The degree of HE increased when the materials were tempered. The HE susceptibility increased from as-Q (18%) over Q&T 1h (50%) to Q&T 2h (52%) for Fe-C-Ti. Similar tendencies were observed for Fe-C-V (26% - 29% - 32%). To elucidate the responsible mechanisms, the H/material interaction was deeply studied.

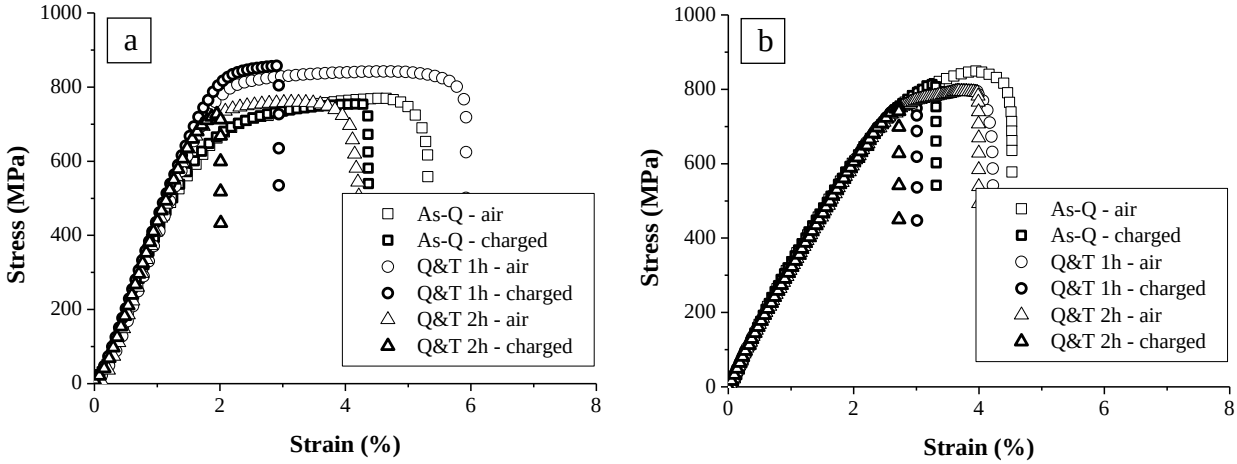

Fig. 4: *Stress-strain curves for (a) Fe-C-Ti and (b) Fe-C-V in the as-Q, Q&T 1h and Q&T 2h condition at a cross-head deformation speed of 5 mm/min of uncharged (air) and H saturated (charged) samples.*

Hydrogen/material interaction

At first, TDS was done on both alloys in the as-Q and Q&T conditions, cf. Fig. 5. Essentially, the first deconvoluted peak was related to H trapped by the martensitic lath boundaries, while the other peaks were correlated to H trapped by the present carbides. The as-Q condition showed only one peak for the Fe-C-V alloy as all carbides were dissolved, while a second peak was observed for the Fe-C-Ti alloy. Large incoherent TiC carbides are not capable of trapping H by electrochemical charging [19], since gaseous H charging at elevated temperature is required to charge these larger particles [25, 26]. Therefore, the cluster of smaller TiC, indicated in Fig. 6, was responsible for the H trapping and the corresponding 2nd TDS peak. When considering the Q&T conditions, additional peaks can be detected linked to the presence of tempered induced carbides. The small TiC and V_4C_3 carbides were capable of trapping a considerable amount of H. The amount of H trapped by carbides decreased with longer tempering time. Consequently, H is assumed to be trapped at the interface between carbides and the matrix since the carbide size was increased and consequently the amount of available interface decreased with tempering time. A more detailed interpretation of these data including activation energies of the deconvoluted peaks can be found elsewhere [19, 20].

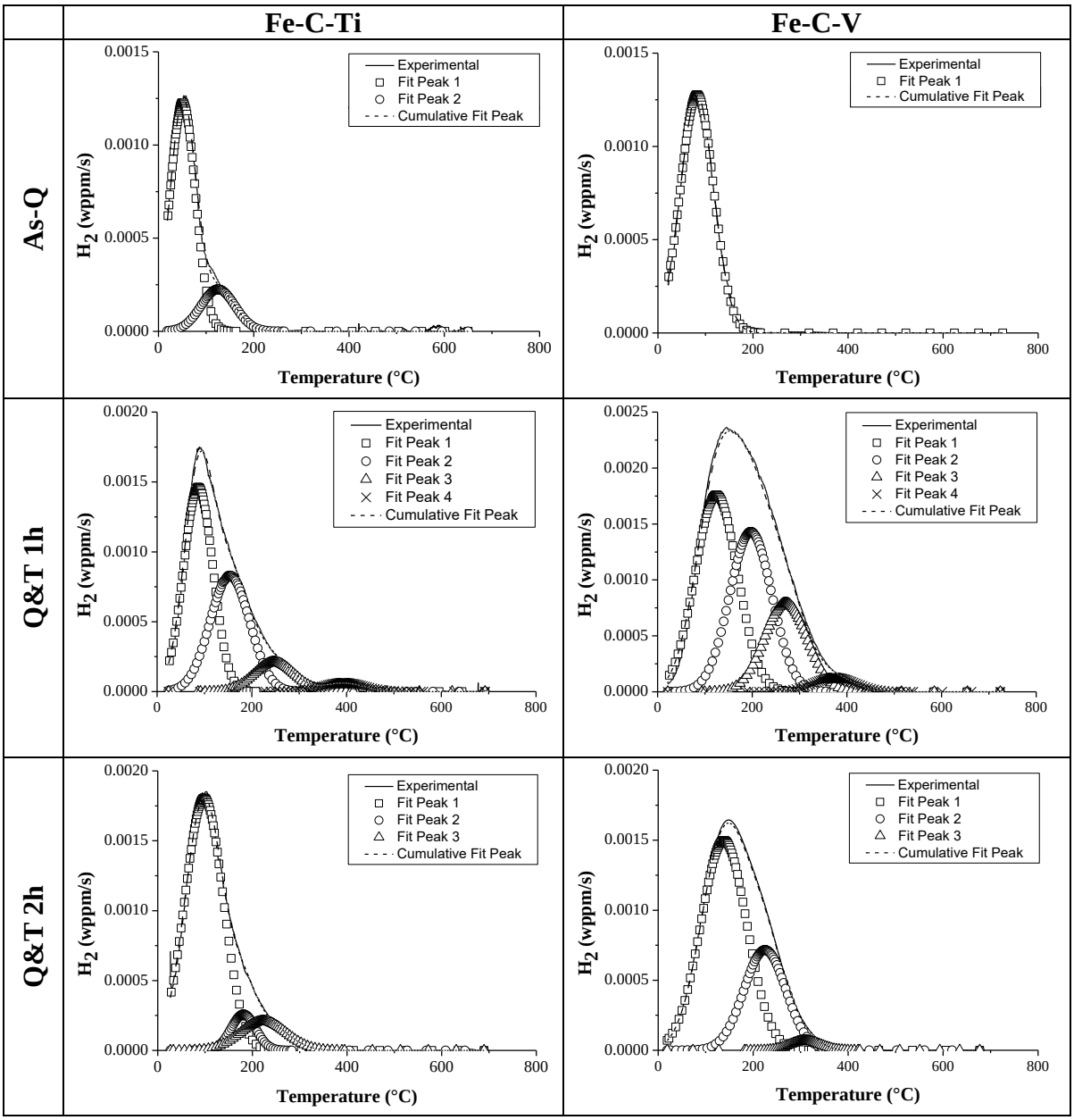

Fig. 5: *TDS curves of Fe-C-Ti and Fe-C-V in the as-Q, Q&T 1h and Q&T 2h condition (heating rate: 600°C/h).*

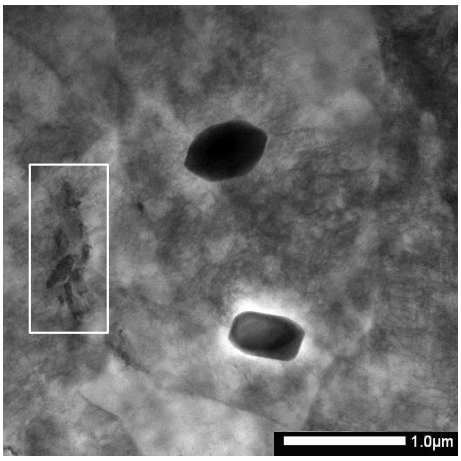

Fig. 6*: STEM bright field image of Fe-C-Ti in the as-Q condition.*

The diffusible and total H content of the H saturated samples was determined by respectively hot and melt extraction and is presented in Fig. 7. The H content clearly increased when the sample was tempered for one hour. Consequently, the microstructural changes that occurred during tempering, mainly the formation of small Ti or V-carbides, provided an important increase in H trapping sites in the material (as experimentally confirmed by the TDS results). However, the Q&T 2h condition clearly showed a different behaviour when both alloys were compared. The H content still increased in the case of Fe-C-Ti, whereas a decrease was detected for the Fe-C-V alloy. These tendencies were similar for the total and diffusible H content.

There is a clear difference between the amount of H as determined by hot extraction, i.e. diffusible H, and the total area under the TDS curve. Indeed, H was able to leave the sample before the TDS measurement. As demonstrated [10, 32], microstructural defects such as dislocations indeed trap H, but loose it before the measurement started, as it took about 1 h to reach a sufficiently low vacuum in the TDS chamber (cf. experimental procedure). This type of H will be defined as "mobile H" [17-20]. During the in-situ tensile tests, however, this mobile H is still present and very relevant for the results obtained during the mechanical tests as discussed below.

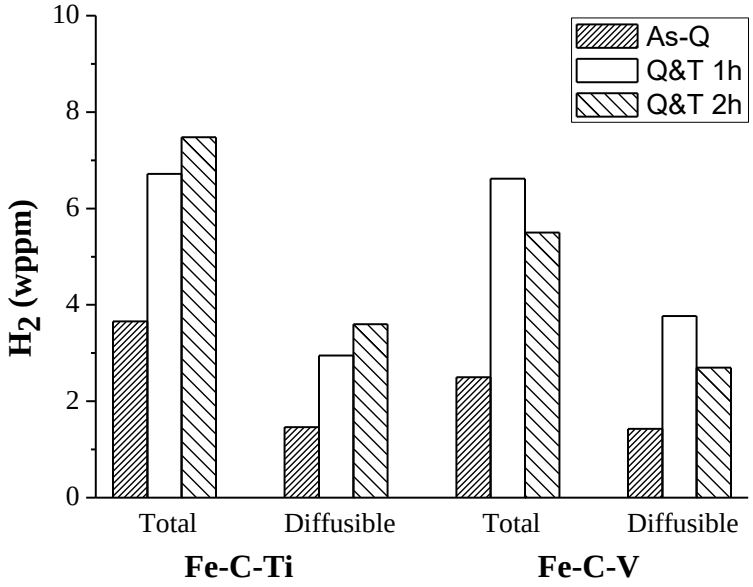

Fig. 7: *The total, diffusible and mobile H contents of the Fe-C-X grades (alloy B) in the as-Q and Q&T condition.*

Although the tempered induced carbides were capable of trapping a significant amount of H, still the degree of HE increased considerably for both alloys. The HE sensitivity for the Fe-C-Ti alloy in the Q&T condition was higher compared to the as-Q state due to the higher amount of total, diffusible and mobile H. The best fit was obtained with the mobile H content, indicating the importance of H trapped by dislocations. The increase in HE was attributed to TiC formed during tempering, which not only increased the H trapping capacity as compared to the as-Q samples, but also introduced weakly trapped H at the elastic stress fields in the matrix surrounding the particle [19, 25]. When the samples were tempered for two hours, the increase in H content was rather limited, resulting in a corresponding small increase in HE%. Since less H was trapped by the carbides when tempered for two hours (cf. TDS results), the elastic strain fields around the coarser TiC were set responsible for the increase in H content and hence the HE%. This specific trap site is however not completely detectable by TDS due

to its experimental operational conditions. Therefore, a rather limited increase in the 1st peak was observed when considering the TDS spectra of the as-Q, Q&T 1h and Q&T 2h condition.

However, different observations were made for the Fe-C-V alloy, since a reduction in H content for the Q&T 2h condition (cf. Fig 7) was detected. This decrease corresponded nicely to the TDS spectra and was correlated to the increase in carbide size, which resulted in lower trapping ability of the V_4C_3 precipitates. However, since only small carbides (< 20 nm) were detected, the elastic strain fields surrounding them did not play a significant role. Consequently, a negligible decrease of the first peak was observed when comparing both tempering conditions. However, the HE% increased when the sample was tempered for two hours, which was correlated to the H saturated carbides in the Q&T 2h samples. The empty carbon sites of V_4C_3 can act as an attractive H trap as well. Subsequently, the presence of H in these carbon vacancies might weaken the interatomic bonding in the brittle V_4C_3 particle, which in their turn induces damage upon charging. Since carbides were larger in the Q&T 2h condition, larger crack lengths can be activated. Moreover, these cracks can also be induced by the applied strain during tensile testing. When considering the TDS spectra, this carbon vacancy H trap is included in the 2nd and 3rd peak. As the total volume of the carbides did not change upon tempering times, this remained present in both Q&T conditions. The observed reduction of the carbide related peaks can still be linked to H trapped at the interface between carbide and matrix, which still showed a decrease with carbide growth. Both carbide trapping sites are thus possible for V_4C_3.
Moreover, the H diffusivity played a determinant role as well. Permeation experiments were therefore performed to determine the H diffusion coefficient (cf. Fig. 8). Tempered induced V_4C_3 precipitates clearly decreased the H diffusivity compared to the as-Q material due to their efficient trapping capacity. The determined diffusion coefficients were about 1.63E-10 m^2/s for as-Q, 5.89E-12 m^2/s for Q&T 1h and 5.39E-11 m^2/s for Q&T 2h. This decrease in H diffusivity was more pronounced for Q&T 1h compared to Q&T 2h since the carbides after two hours tempering were less capable of trapping H as shown by TDS in Fig. 5. Consequently, although the H content decreased for Q&T 2h, the H diffusivity increased, which additionally explained the increased HE susceptibility for Q&T 2h as well.

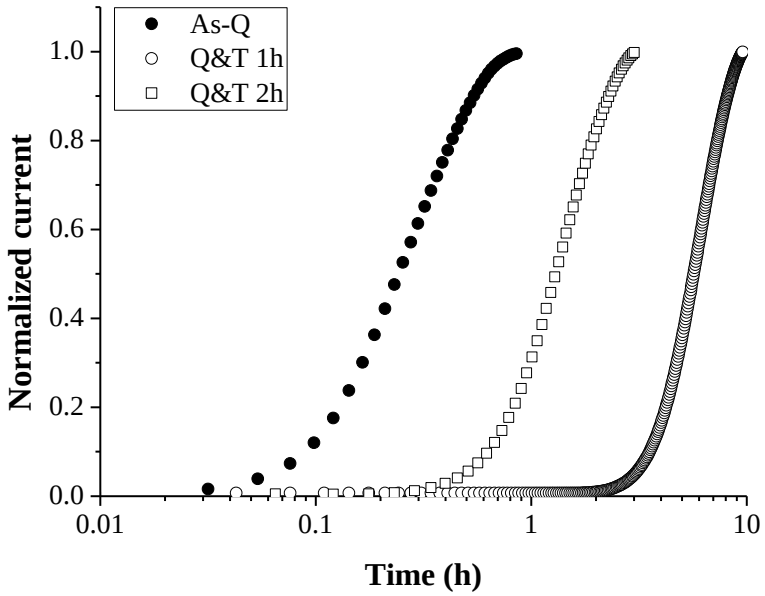

***Fig. 8**: Permeation curves on Fe-C-V in the as-Q, Q&T and Q&T 2h condition.*

The impact of Ti and V based carbides/carbo-nitrides in a ferritic matrix

Since size and coherency of the carbides played an important role in their trapping ability for martensitic materials, the effect of Ti and V based precipitates was evaluated in a different matrix as well. A ferritic microstructure was aimed for as this phase facilitates the analysis and interpretation of the data. While carbides were introduced during tempering for the Q&T condition, carbides were, in this case, induced during the ferrite formation. Austenitizing was performed at 1250 for 30 minutes to dissolve the present carbides from casting and rolling. Subsequently, a controlled precipitation of carbides together with ferrite formation took place at an isothermal temperature of 800°C for 10 minutes. Finally, the materials were air cooled to obtain a ferritic microstructure together with well-designed Ti and V based carbides. This matrix allows investigating the impact of carbides without the presence of a high dislocation density complicating microstructural characterization. Therefore, the sample geometry was also modified (cf. Fig. 9), i.e. a notch with stress concentration of 4.2 was introduced to control fracture initiation to facilitate further microstructural analysis.

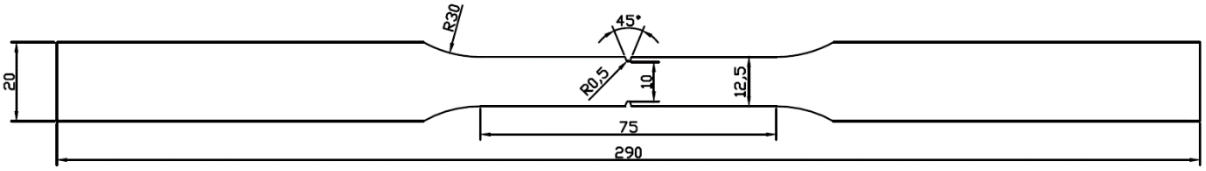

***Fig. 9**: Tensile sample geometry in mm.*

The present carbides showed a different morphology compared to the ones observed in the as-Q and Q&T microstructures. Precipitates were significantly larger due to the softer matrix in which they were embedded and the respectively longer and higher annealing time and temperature. STEM images were taken and are presented in Fig. 10. While only pure TiC and V_4C_3 particles were observed in the martensitic materials, different types of carbides were seen in this ferrite matrix. The small coherent carbides still showed a similar morphology, whereas the larger incoherent particles were enriched with N resulting in V and Ti based carbo-nitrides instead of pure carbides.

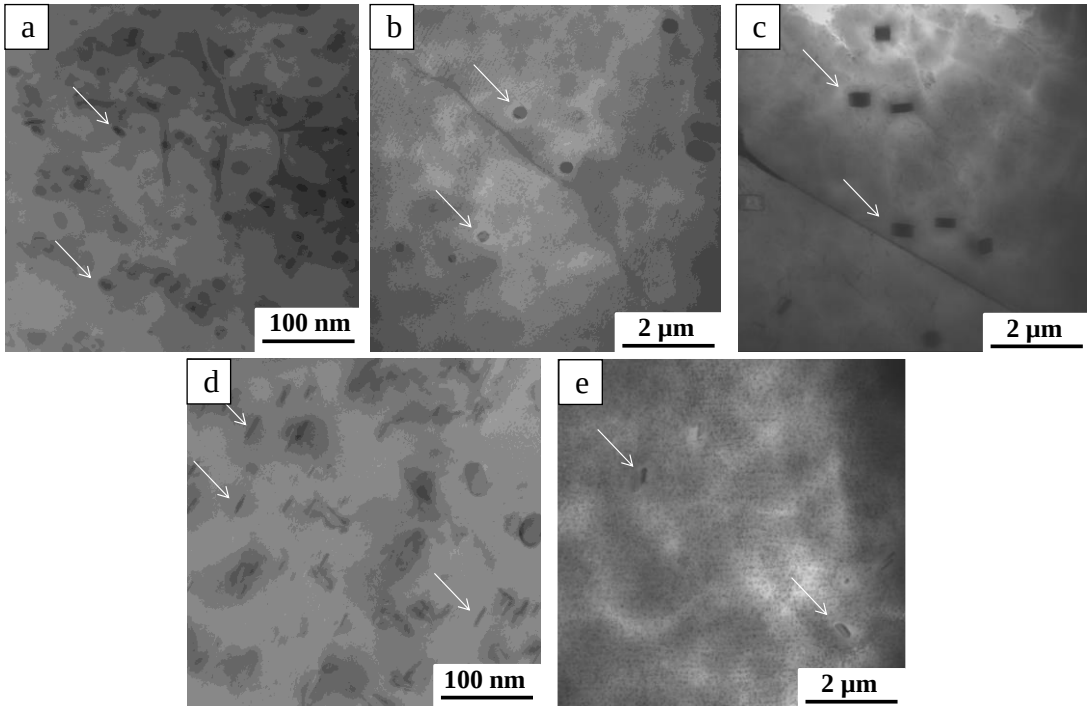

***Fig. 10**: STEM images of a) small coherent TiC, b) larger spherical Ti(C,N), and c) square Ti(C,N) in Fe-C-Ti and d) small coherent V_4C_3, and e) larger incoherent V(C,N) in Fe-C-V.*

The stress-strain curves for the ferritic Ti and V alloy are presented in Fig. 11. A significantly ductility drop was observed. At first, the tests in air showed a lower strength level than the martensitic grades due to the softer ferrite matrix. Also, the materials showed more ductility compared to the as-Q and Q&T alloys since similar strain levels were obtained whereas a notch is present in the ferritic tensile samples, which was also linked to the more ductile behaviour of the ferrite matrix. The Fe-C-V alloy showed a higher strength level which can be correlated to the higher amount of C which was dissolved during austenitizing (cf. Fig. 2). This reasoning can also explain the lower strain level obtained for the Fe-C-V material. The degree of HE increased when comparing with the as-Q and Q&T conditions for both alloys. A HE degree of 53% was determined for Fe-C-Ti, whereas the Fe-C-V lost about 62% of its ductility. To understand these results, the H/material interaction was studied in detail.

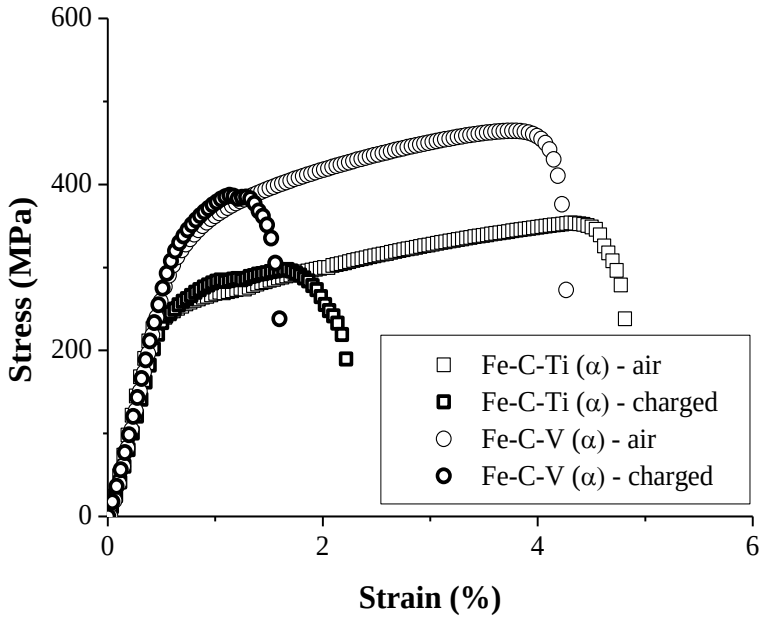

Fig. 11: *Stress-strain curves for Fe-C-Ti and Fe-C-V in annealed condition at a cross-head deformation speed of 0.05 mm/min of uncharged (air) and H saturated (charged) samples.*

TDS was performed to verify whether the carbides were able to trap H. An improved TDS apparatus was used allowing the measurement to start about one minute after H charging, similar as hot/melt extraction. Consequently, all H was detected and the resulting TDS spectra contain more H compared to the previous results, for which a TDS device was used requiring one hour establishing vacuum in the analysis chamber. Therefore, no comparison between the obtained TDS spectra on H content is possible. However, low amounts of H were detected as illustrated in Fig. 12 and 13. To clearly visualize the carbide related peak, the spectra obtained at a heating rate of 1200°C/h were shown since as such the distinction between the peaks is easier to observe. The first peak was correlated to H trapped at the grain boundaries and dislocations. A clear though small 2nd peak linked to Ti and V based particles was detected as well, while considerably more H was present in the Fe-C-V alloy. Significantly less H was trapped by the present carbides compared to the Q&T conditions (cf. Fig. 5), which was correlated with their larger sizes and more incoherent nature due to the softer matrix in which they are embedded (cf. Fig. 3 and 10).

The amount of diffusible and total H was determined by the same hot/melt extraction device. All considered microstructures were presented in Fig. 13. Less H was trapped by the annealed samples, which was linked to the ferritic matrix and the larger particles. Remarkably, the total amount of H was larger for Fe-C-Ti, while the diffusible H content was about half the amount detected for Fe-C-V. The latter matched nicely to the TDS results where similar H contents

were detected. Apparently, the Fe-C-Ti alloy contained trapping sites which can only be detected by melting the samples. Since the larger spherical and square Ti(C,N) cannot trap H by electrochemical H charging [19, 26], the undissolved Ti based precipitates or the larger ones formed during the heat treatment are presumably responsible for this observation. Further analysis is needed to confirm this hypothesis, for which we would like to refer to reader to [33, 34].

The diffusible H content clearly played a determinant role in the HE degree since the HE susceptibility was higher for the Fe-C-V alloy compared to the Fe-C-Ti alloy. Moreover, H which is released above 900°C (cf. TDS results) is considered to be trapped irreversibly and not to influence the mechanical properties anymore. The higher degree of HE for the annealed condition compared to the as-Q and Q&T conditions can clearly not solely be linked to the H content (cf. Fig. 13). Here, the H diffusivity, which is considerably higher in ferrite compared to martensite [15], can be held responsible since a synergetic effect of both the H amount and H diffusion/mobility plays a role, as illustrated by the authors [15-20].

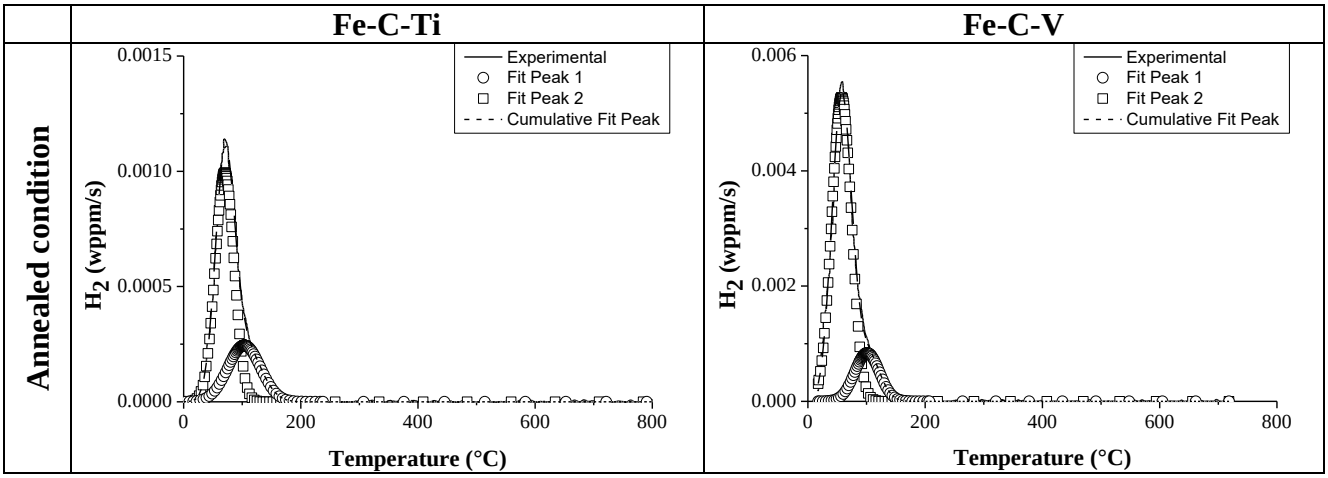

Fig. 12: *TDS spectra determined by a modified TDS device of the Fe-C-Ti and Fe-C-V alloy in the annealed condition (heating rate: 1200°C/h).*

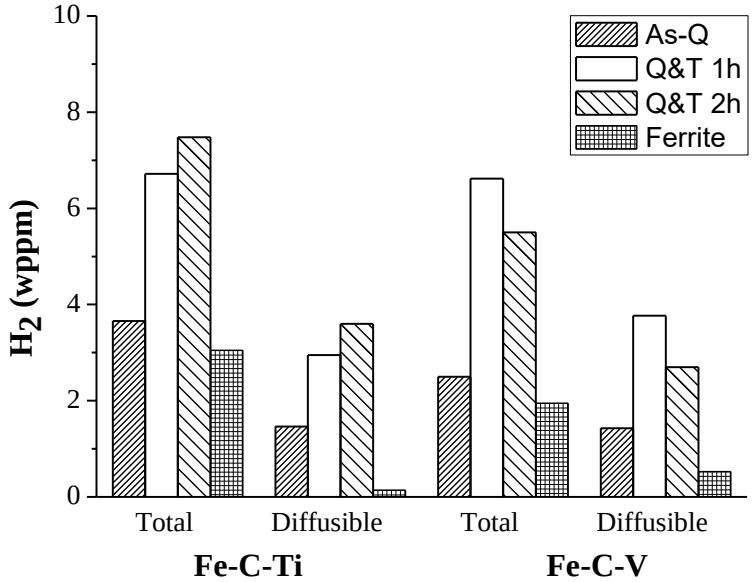

Fig. 13: *Hot and melt extraction results for Fe-C-Ti and Fe-C-V in the as-Q, Q&T 1h, Q&T 2h and the annealed condition.*

To verify whether carbide addition is beneficial to increase the resistance against H induced mechanical degradation, these ferritic microstructures were characterized. The fracture surface was studied by SEM as presented in Fig. 14. A typical HE phenomenon of fish eyes was observed. An inclusion is present at the center and further fracture occurs in a pattern radiating away from the pupil. The composition of the precipitate was similar to the large incoherent Ti(C,N) particles, indicating a detrimental role of these precipitates. Further analysis is ongoing to fully comprehend their role [34].

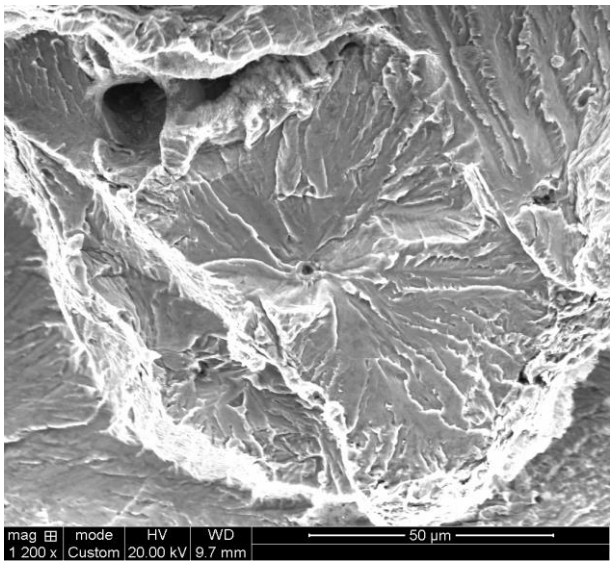

Fig. 14*: Fracture surface of the tensile sample of the Fe-C-Ti alloy, revealing a fish eye with a Ti(C,N) inclusion as initiation site.*

Conclusion

Two lab cast Fe-C-X materials (with X = Ti or V) were investigated in both the as-Q, Q&T 1h, Q&T 2h and annealed ferritic condition. The effect of the present carbides on the H trapping and H induced mechanical degradation was evaluated. When considering the martensitic materials, the tempered induced carbides trapped a significant amount of H as observed by TDS. The HE susceptibility increased when tempering was applied and with tempering time. For the Fe-C-Ti alloy, this increase was correlated with the amount of H. Tempered induced carbides trapped a significant amount of H and the content trapped by TiC decreased for longer tempering times, indicating H was trapped at the interface between the carbides and the matrix. However, the H content further increased with tempering due to the elastic stress fields around the larger TiC. This was set responsible for the increased HE sensitivity. For the Fe-C-V alloy, two trap sites were observed, i.e. at the interface between the carbides and matrix and at the carbon vacancies inside the V_4C_3 particles. This was concluded since the degree of HE increased when two hours of tempering was applied while the H content decreased. Carbides with sizes less than 10 nm are considered to be very efficient to trap H in both alloys.

Lower amounts of H were detected in the annealed ferritic condition and the Ti and V based carbides were able to trap only a limited amount of H, probably due to their larger size. Hence, their beneficial impact on the HE resistance is negligible. Therefore, the considerable H induced ductility loss was linked to the higher H diffusivity in a ferritic matrix compared to a martensitic matrix. Additionally, analysis of the surface fracture showed a fish eye with a Ti carbo-nitride as the initiation site, indicating the detrimental effect of the larger incoherent carbo-nitrides in terms of H induced mechanical degradation.

Acknowledgements

The authors thank the Special Research Fund (BOF), UGent (BOF15/BAS/06) and the Agency for Innovation by Science and Technology in Flanders (IWT) for support (Project nr SB111205), V. Bliznuk and E. Wallaert for the TEM images. The authors also acknowledge the technicians and staff working at the hydrogen laboratory at ArcelorMittal R&D Gent and the Department of Materials, Textiles and Chemical Engineering, UGent, for their help with the experiments and sample preparation.

References

1. M. Loidl, Adv Mat Process, **169** (2011) 22.
2. T.B. Hilditch, S.B. Lee, J.G. Speer, D.K. Matlock, SAE Technical Paper, (2003) http://dx.doi.org/10.4271/2003-01-0525.
3. M. Koyama, E. Akiyama, Y.K. Lee, D. Raabe, K. Tsuzaki, Int Journal of H Energy, **42** (2017) 12706.
4. T. Depover, D. Pérez Escobar, E. Wallaert, Z. Zermout, K. Verbeken, Int Journal of H Energy, **39** (2014) 4647.
5. J.A. Ronevich, J.G. Speer, D.K. Matlock, SAE Int Journal Mat Man, **3** (2010) 255.
6. M. Koyama, C. Tasan, E. Akiyama, K. Tsuzaki, D. Raabe, Acta Mat, **70** (2014) 174.
7. H. Yu, J.S. Olsen, A. Alvaro, V. Olden, J. He, Z. Zhang, Eng Fract Mech, **157** (2016) 56.
8. D. Pérez Escobar, K. Verbeken, L. Duprez, M. Verhaege, Mat Sci and Eng A, **551** (2012) 50.
9. D. Pérez Escobar, C. Miñambres, L. Duprez, K. Verbeken, M. Verhaege, Corrosion Science, **53** (2011) 3166.
10. D. Pérez Escobar, T. Depover, E. Wallaert, L. Duprez, K. Verbeken, M. Verhaege, Acta Mat, **60** (2012) 2593.
11. T. Depover, E. Wallaert, K. Verbeken, Mat Sci and Eng A, **649** (2016) 201.
12. A. Laureys, T. Depover, R. Petrov, K. Verbeken, Int Journal of H Energy, **40** (2015) 16901.
13. A. Laureys, T. Depover, R. Petrov, K. Verbeken, Materials Characterization, **112** (2016) 169.
14. W.H. Johnson, Proc Royal Society London, **23** (1875) 168
15. T. Depover, E. Wallaert, K. Verbeken, Mat Sci and Eng A, **664** (2016) 195.
16. T. Depover, E. Van den Eeckhout, K. Verbeken, Mat Sci and Tech, **32** (2016) 1625.
17. T. Depover, K. Verbeken, Mat Sci and Eng A, **669** (2016) 134.
18. T. Depover, K. Verbeken, Int Journal of H Energy, **41** (2016) 14310.
19. T. Depover, K. Verbeken, Corrosion Science, **112** (2016) 308.
20. T. Depover, K. Verbeken, Mat Sci and Eng A, **675** (2016) 299.
21. T. Asaoka, G. Lapasset, M. Aucouturier, P. Lacombe, Corros NACE, (1978), 39.
22. H.G. Lee, J.Y. Lee, Acta Met, **32** (1984) 131.
23. G.M. Pressouyre, I.M. Bernstein, Met Trans A, **9A** (1978) 1571.
24. F.G. Wei, T. Hara, K. Tsuzaki, Met Mat Trans B, **35B** (2004) 587.
25. F.G. Wei, K. Tsuzaki, Met Mat Trans A, **37A** (2006) 331.
26. D. Pérez Escobar, E. Wallaert, L. Duprez, A. Atrens, K. Verbeken, Met Mat Int, **19** (2013) 741.
27. H. Asahi, D. Hirakami, S. Yamasaki, ISIJ Intl, **43** (2003) 527.
28. D. Li, R.P. Gangloff, J.R. Scully, Met Mat Trans A, **35** (2004) 849.
29. G.L. Spencer, D.J. Duquette, The role of V carbide traps in reducing the HE susceptibility of high strength alloy steels, Watervliet, N.Y., (1998).

30. T. Depover, O. Monbaliu, E. Wallaert, K. Verbeken, Int Journal of H Energy, **40** (2015) 16977.
31. F.G. Wei, T. Hara , K. Tsuzaki, “Nano-precipitates design with H trapping character in high strength steels”, in Proc of the Int H Conf, Jackson, ASM Int, Jackson, WY (2008) pp. 448-455.
32. T. Depover, K. Verbeken, “The role of dislocation mobility on the hydogen induced mechanical degrdation of Fe-C-X alloys”, in Proc of the Eurocorr Conf, Prague, Czech Republic (2017), submitted
33. A. Laureys, L. Claeys, T. De Seranno, T. Depover, R. Petrov, K. Verbeken, “Characterization of H induced cracking in ferritic Fe-C-Ti and Fe-C-V alloys”, in Proc of the Int H Conf, Jackson, ASM Int, Jackson, WY (2016).
34. A. Laureys, L. Claeys, T. De Seranno, T. Depover, R. Petrov, K. Verbeken, unpublished results.